POLITECNICO DI TORINO
Repository ISTITUZIONALE

Understanding polarization with gratings tilted to crystal axes: towards circularly-polarized VCSELs

(Article begins on next page)

05 February 2025

Understanding polarization with gratings tilted to crystal axes: towards circularly-polarized VCSELs

V. Torrelli[1,2], L. Miri[1], M. D'Alessandro[1,2], A. Gullino[2], R. de Gennaro[1], W. Elsässer[2,3,4], A. Tibaldi[1] and P. Debernardi[2]

1. Department of Electronics and Telecommunications (DET), Politecnico di Torino, Italy
2. Istituto di Elettronica e di Ingegneria dell'Informazione e delle Telecomunicazioni (IEIIT) del Consiglio Nazionale delle Ricerche (CNR), Politecnico di Torino, Italy
3. Institute of Applied Physics, Technische Universität Darmstadt, Schlossgartenstrasse 7, 64289 Darmstadt, Germany
4. School of Physics, Trinity College Dublin, Dublin 2, Ireland
valerio.torrelli@polito.it

Abstract—We demonstrate that tailored anisotropies in VCSELs give rise to elliptically-polarized light. This can be achieved exploiting the intrinsic electro-optic anisotropy and a tilted surface grating with respect to crystallographic axes, targeting circular polarization with conventional grating-VCSEL technology.

Keywords—VCSELs, gratings, circular polarization, elliptical polarization, chirality, anisotropies, electro-optic effect

I. Introduction

At early stages of vertical-cavity surface-emitting lasers (VCSELs) history, polarization instability and switching led to the need for polarization control. Eventually, perfectly stable linear polarization was achieved via surface gratings etched on the outcoupling facet of the device [1].

Nowadays, many applications like atomic clocks and quantum gyroscopes [2] require lasers emitting circularly-polarized light. Traditionally, this is achieved with a linearly-polarized VCSEL combined with a quarter waveplate, resulting in a cumbersome and bulky setup. Proposed monolithic solutions are based on the introduction of chiral layers [2]. Starting from this preliminary idea, this work aims at pushing further the structure chirality, combining the effects of the intrinsic VCSEL anisotropies along the crystalline axes and a tilted surface grating. This allows to obtain monolithic devices emitting circularly-polarized light, exploiting the well-established manufacturing process consolidated for linear polarization control.

We exploit this concept to explain the results in [3], where a VCSEL with a grating tilted of 45° to the crystalline axes is analyzed by means of a linear polarizer for quantum communication purposes.

II. Results and Discussions

For our analysis, we investigate a standard 850 nm AlGaAs VCSEL featuring a λ-cavity, a 20-pairs top p-doped distributed Bragg reflector (DBR) and a 35-pairs bottom n-doped DBR. The doping levels in the structure are $3 \cdot 10^{18}$ cm^{-3} for the first 15 pairs of the top DBR and for the substrate and $2 \cdot 10^{18}$ cm^{-3} for the remaining top and bottom DBRs. Furthermore, a subwavelength grating (SWG) between GaAs and air is placed

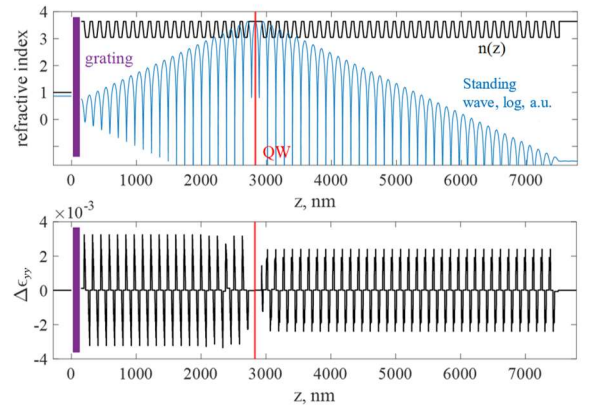Fig. 1. Top: refractive index profile (black) and supported standing wave (blue) obtained for a grating thickness of $t = 147$ nm and $\theta = 53°$. Bottom: dielectric constant modification profile along the y-direction induced by the electro-optic anisotropy.

at the outcoupling facet, featuring a filling factor of 0.5 and a spatial period of 150 nm. A parametric campaign is performed for the grating thickness t and the tilting angle ϕ to the GaAs crystalline axes, chosen as (x, y) reference system. The refractive index profile, together with the supported standing wave, is reported in Fig. 1 (top).

The electro-optic effect is accounted for by modifying the dielectric constant profile $\epsilon(z)$ along x and y as [4]

$$\Delta\epsilon_{xx(yy)} = +(-)n^4 r_{41} \mathcal{E}_z, \tag{1}$$

where n is the refractive index, r_{41} is the Pockels coefficient and $\mathcal{E}_z$ is the electrostatic field. The values of r_{41} are taken as 1.6 [5] and 0.78 pm/V [6] for GaAs and AlAs, respectively. When considering $Al_x Ga_{1-x} As$, a linear behavior in $x \in [0,1]$ is assumed. The electrostatic field profile is obtained via a 1D drift-diffusion simulation [7] of the VCSEL with an applied bias of 3 V. The corresponding $\Delta\epsilon_{yy}$ is reported in Fig. 1 (bottom).

Neglecting transverse variations, not relevant from the polarization standpoint, electromagnetic simulations have been performed using a vectorial generalization of our 1D VCSEL ELectroMagnetic Suite (VELMS) [8], where the anisotropic dielectric constant profiles $\epsilon_{xx(yy)}(z)$ are taken as input.
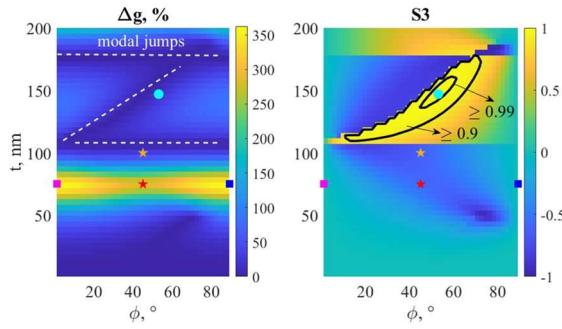
Fig. 2. Left: color density plot of the threshold gain difference Δg [%] for varying grating thickness t and angle ϕ. White dashed lines represents regions where $\Delta g = 0$. Right: corresponding S_3 of the lasing mode, highlighting regions of the parameter space where it exceeds 0.9 and 0.99. Markers represent specific cases of interest.

Without the grating, the two polarization modes feature a negligible threshold gain difference of $0.12~\text{cm}^{-1}$ and a typical frequency split of 14 GHz. The grating is treated according to rigorous coupled wave analysis [9] to extrapolate its transmission matrix. The effect of the grating on the modal features is studied by varying $t \in [0, 200]$ nm and $\phi \in [0, 90]°$, focusing on the threshold gain difference defined through the lasing and superior threshold gains g_l and g_s as

$$\Delta g = 100 \cdot (g_s - g_l)/g_l. \tag{2}$$

This analysis also concentrates on the Stokes parameter S_3 of the lasing mode, representing the degree of circular polarization of the emitted light [10]. In general $-1 \leq S_3 \leq 1$, where $S_3 = \pm 1$ represents clockwise and counterclockwise circular polarizations, $S_3 = 0$ linear polarization and in-between values elliptical polarizations. Δg and S_3 are displayed in Fig. 2. In correspondence of the white dashed lines, representing $\Delta g = 0$ trajectories, one can notice a sudden jump of S_3, indicating a change in lasing polarization.

The transverse modes emitted by standard VCSELs feature different spatial distributions. From the vectorial field analysis, each of them displays two polarized states sharing the same shape. Aiming at ensuring the emission of a specific polarization mode, a small Δg is required, with the spatial hole burning playing no role in polarization mode competition. Aiming at maximizing $|S_3|$, the cyan circle represents fully circularly-polarized light ($S_3 = 1$) with an acceptable $\Delta g = 18$ %.

Consider now the complex emission unit vector of the lasing optical field $\hat{E} = E_x \hat{x} + E_y \hat{y}$ for a certain (t, ϕ) combination impinging on a linear polarizer whose axis is tilted to $\hat{x}$ of γ. The light intensity coming out of the polarizer can be obtained as:

$$I_{out}(\gamma) = \left| \hat{E} \cdot (\hat{x} \cos \gamma + \hat{y} \sin \gamma) \right|^2. \tag{3}$$

To better understand particular cases of (3), consider an impinging linear polarization oriented along a certain angle α, then $I_{out} = 1$ for $\gamma = \alpha + k\pi$, while $I_{out} = 0$ for $\gamma = \alpha + \frac{\pi}{2} + k\pi, k \in \mathbb{Z}$. On the other hand, for impinging circular polarization, $I_{out} = 0.5~\forall \gamma$. For elliptical polarization, $I_{out}(\gamma)$ varies without reaching zero. Magenta and blue squares in Fig. 2 represent standard usages of SWGs, maximizing Δg and achieving perfectly linearly-polarized light at the output ($S_3 = 0$). The corresponding intensity of the linear polarizer is shown
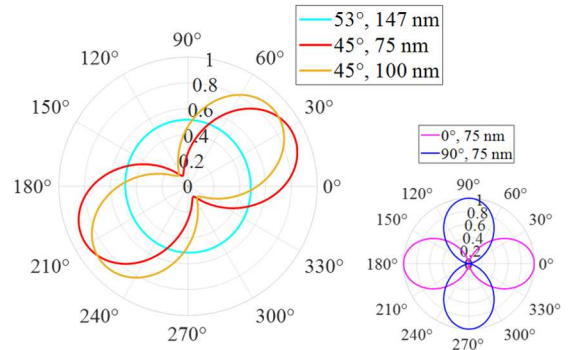

Fig. 3. Left: output intensity of the linear polarizer as a function of the polarizer angle γ for impinging elliptical (red and orange curves) and circular (cyan) lasing polarizations. Right: corresponding results for impinging linear polarizations oriented along $\hat{x}$ (magenta) and $\hat{y}$ (blue).

in Fig. 3 (right), featuring zeros (closing the "8" shape). On the other hand, similar values of t compared to the standard case but with $\phi = 45°$ lead to elliptical polarization with a worse polarization control (lower Δg). Red and orange stars in Fig. 2 denote this scenario, with the output of the linear polarizer shown in Fig. 3 (left). This establishes that the corresponding results in [3] showcase the first experimental demonstration of elliptically-polarized light obtained through a tilted grating. Finally, the cyan circle case of perfectly circularly-polarized light displays a constant output intensity of 0.5 in Fig. 3 (left), as expected from (3).

III. CONCLUSIONS

We demonstrated how tilted anisotropies in VCSELs can generate elliptical polarizations, achievable by the interaction of intrinsic anisotropies and a misaligned grating. The output polarization can be tailored by changing either the electric field within the device, influenced by technological parameters like grading and doping, or by changing the SWG. Such a simple solution does not require a modification of SWG technology, thus paving the way for circularly-polarized VCSELs.

IV. ACKNOWLEDGMENT

REFERENCES

[1] P. Debernardi, G. P. Bava, IEEE J. Select. Topics Quantum Electron. 9, 905 (2003).

[2] X. Jia, et al., Optica 10, 1093 (2023).

[3] M. Zimmer, M. Birkhold, M. Jetter, P. Michler, Vertical-Cavity Surface-Emitting Lasers XXVIII, (SPIE, 2024), vol. PC12904, p.PC1290402.

[4] P. Debernardi, G. Bava, Physica S. S. A 188, 967 (2001).

[5] G. Sinatkas, T. Christopoulos, O. Tsilipakos, E. E. Kriezis, J. Appl. Phys. 130 (2021).

[6] S. Adachi, ed., Properties of Aluminium Gallium Arsenide, EMIS Datareviews Series (INSPEC, London, 1993).

[7] A. Gullino, A. Tibaldi, F. Bertazzi, M. Goano, P. Debernardi, MDPI Appl. Sci. 11, 6908 (2021).

[8] V. Torrelli, et al., IEEE Photon. J. 16, 0600507 (2024).

[9] M. G. Moharam, T. K. Gaylord, J. Opt. Soc. Amer. 71, 811 (1981).

[10] A. Molitor, P. Debernardi, S. Hartmann, W. Elsässer, Opt. Lett. 38, 4777 (2013).